

Gate-tuned superconductor-insulator transition in (Li,Fe)OHFeSe

B. Lei,¹ Z. J. Xiang,¹ X. F. Lu,¹ N. Z. Wang,¹ J. R. Chang,¹ C. Shang,¹ A. M. Zhang,⁵ Q. M. Zhang,^{5,6} X. G. Luo,^{1,4} T. Wu,^{1,4} Z. Sun,^{3,4} and X. H. Chen^{1,2,4,*}

¹Hefei National Laboratory for Physical Science at Microscale and Department of Physics, and Key Laboratory of Strongly-coupled Quantum Matter Physics, Chinese Academy of Sciences, University of Science and Technology of China, Hefei, Anhui 230026, China

²High Magnetic Field Laboratory, Chinese Academy of Sciences, Hefei, Anhui 230031, China

³National Synchrotron Radiation Laboratory, University of Science and Technology of China, Hefei, Anhui 230026, China

⁴Collaborative Innovation Center of Advanced Microstructures, Nanjing University, Nanjing 210093, China

⁵Department of Physics, Beijing Key Laboratory of Opto-electronic Functional Materials and Micro-nano Devices, Renmin University of China, Beijing 100872, China

⁶Department of Physics and Astronomy, Collaborative Innovation Center of Advanced Microstructures, Shanghai Jiao Tong University, Shanghai 200240, China

(Received 4 November 2015; published 1 February 2016)

The antiferromagnetic (AFM) insulator-superconductor transition has always been a center of interest in the underlying physics of unconventional superconductors. However, in the family of iron-based high- T_c superconductors, no intrinsic superconductor-insulator transition has been confirmed so far. Here, we report a first-order transition from superconductor to AFM insulator with a strong charge doping induced by ionic gating in the thin flakes of single crystal (Li,Fe)OHFeSe. The superconducting transition temperature (T_c) is continuously enhanced with electron doping by ionic gating up to a maximum T_c of 43 K, and a striking superconductor-insulator transition occurs just at the verge of optimal doping with highest T_c . A phase diagram of temperature-gating voltage with the superconductor-insulator transition is mapped out, indicating that the superconductor-insulator transition is a common feature for unconventional superconductivity. These results help to uncover the underlying physics of iron-based superconductivity as well as the universal mechanism of high- T_c superconductivity. Our finding also suggests that the gate-controlled strong charge doping makes it possible to explore novel states of matter in a way beyond traditional methods.

DOI: [10.1103/PhysRevB.93.060501](https://doi.org/10.1103/PhysRevB.93.060501)

The quantum phase transition between a Mott insulator with antiferromagnetism and a superconductor can be induced by doping charge carriers in high- T_c cuprate superconductors [1]. For the best characterized organic superconductors of κ -(BEDT-TTF)₂X (X = anion), a first-order transition between an antiferromagnetic insulator and a superconductor can be tuned by applied external pressure or chemical pressure [2–4]. Also, the superconducting state can be directly developed from an antiferromagnetic insulator by the application of pressure in Cs₃C₆₀ [5]. The resemblance of these phase diagrams hints at a universal mechanism governing the unconventional superconductivity in close proximity to antiferromagnetic insulators. For the iron-based high- T_c superconductors, however, the superconductivity evolves from an antiferromagnetic bad metal by doping charge carriers [6–8], and the information of intrinsic superconductor-insulator transition is still lacking.

Phase diagrams have been extensively studied in the iron-based superconductors with a large range of carrier doping, while such investigations are very limited in the iron chalcogenides because the known FeSe-derived superconductors are not suitable to study the underlying physics due to reasons mentioned in the Ref. [9], such as phase separation in K_xFe_{2-y}Se₂ [10]. On the other hand, controllable manipulation of various phases through the gate-tunable charge doping has been confirmed to lead to a new device paradigm for future material sciences and technologies [11–14]. Recently, we find an ionic liquid that can dope charge carriers with driving Li

ions in the layered 1T-TaS₂ controlled by a gate electric field in the extreme charge-carrier-concentration limit [15], which is different from the ionic liquid used for the electron-double-layer surface gating. Such ionic liquid provides us a chance to map out the phase diagram of the layered iron-chalcogenide superconductors. The newly discovered FeSe-derived superconductor (Li_{0.8}Fe_{0.2})OHFeSe [9] is suitable for mapping out a carrier-doping phase diagram by ionic gating due to its stability in air and layered structure. In this Rapid Communication, we show the variation of transport behavior with carrier concentration controlled by gate electric field in the thin flakes of the layered high- T_c superconductor (Li,Fe)OHFeSe. We have successfully achieved the continuous gate voltage controlling of the electronic phases in (Li,Fe)OHFeSe with a setup of ionic field-effect transistor (iFET). A remarkable superconductor-insulator transition occurs with the carrier doping, bearing a resemblance to phase diagrams of many other unconventional superconductors.

Electrical transport properties of exfoliated single-crystalline (Li,Fe)OHFeSe thin flakes with a typical thickness of ~200 nm were systematically studied upon applying a gate voltage (V_g). A liquid polymer electrolyte (LiClO₄/PEO) was chosen to serve as the dielectric through which the electric field was established. The details of device preparation are described in the Supplemental Material [16]. When a continuously swept positive gate voltage is applied at 330 K, the resistance of (Li,Fe)OHFeSe thin flake starts to drop gradually when V_g is ramped up to about 2.5 V, and reaches a minimum at $V_g \simeq 4$ V, then increases rapidly and is enlarged by one order of magnitude as V_g approaches 5 V as shown

*Corresponding author: chenxh@ustc.edu.cn

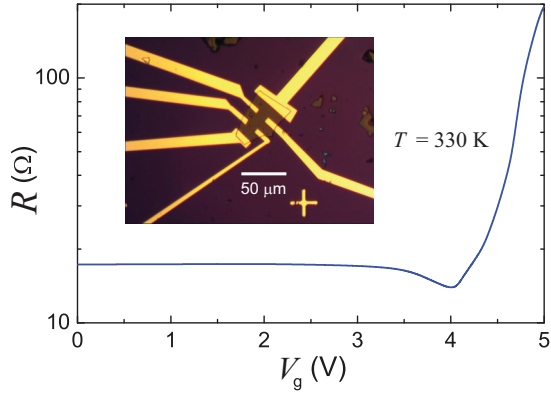


FIG. 1. Gate-voltage dependence of the resistance for a (Li,Fe)OHFeSe crystal flake (with a thickness of $\simeq 200$ nm) during a continuous upswEEP at 330 K. The V_g sweep rate is 1 mV s^{-1} . The inset shows an optical image of the iFET device used in our measurements.

in Fig. 1. This nonmonotonic behavior hints that an unusual change takes place around $V_g = 4$ V, separating the low-resistive state and the high-resistive one.

To investigate the nature of this unusual change, we measured the temperature dependence of resistance of (Li,Fe)OHFeSe with various V_g applied (see Fig. 2). At $V_g = 0$ V, this sample is superconducting (SC) with midpoint critical temperature $T_c^{\text{mid}} = 24.4$ K. The zero-resistance temperature $\simeq 20$ K is consistent with magnetic susceptibility measurement (see Supplemental Material [16]). With the increase of V_g , T_c^{mid} continuously shifts up and the normal-state resistance decreases until a critical gate voltage $V_g^C = 3.9$ V. At $V_g = V_g^C$ the sample exhibits a maximum of $T_c^{\text{mid}} = 43.4$ K, the same value as we have observed in polycrystalline (Li_{0.8}Fe_{0.2})OHFeSe [9,17]. Beyond V_g^C an insulating behavior immediately sets in and the SC transition completely disappears, as indicated by the R - T curve at $V_g = 4.0$ V. The further increase of V_g promptly strengthens the insulating behavior, and finally pushes the low-temperature resistance to a magnitude of more than five orders larger than the normal-state resistance of the SC phase. In all devices we studied, T_c^{mid} at

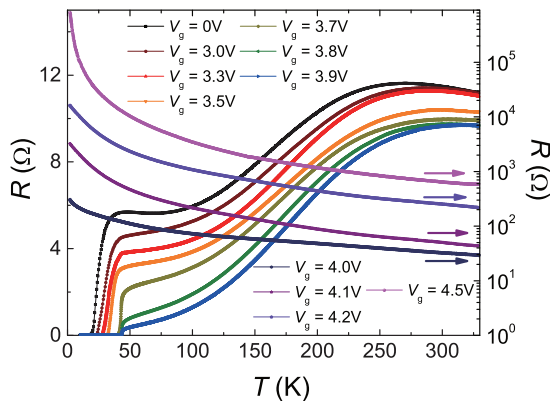


FIG. 2. Temperature-dependent resistance of a (Li,Fe)OHFeSe iFET at various gate voltages. The longitudinal resistance was measured from 2 to 330 K at different gate biases ranging from 0 to 4.5 V.

$V_g = 0$ V varies from 22 to 36 K (see Supplemental Material, Fig. S2b [16]), and V_g^C also ranges from 3.6 to 4.0 V, but the overall evolving behavior upon gating always remains the same. In particular, both the optimal $T_c^{\text{mid}} = 43.4$ K and the sharp transition from the SC to insulating behavior were repeated in each device. No mixed state of SC phase with optimal T_c and the insulating phase has ever been observed.

Considering the sharpness of the SC transition (transition width < 1 K) in the vicinity of optimal superconductivity [see Fig. S4(a) in Supplemental Material [16]], and the absence of residual superconductivity in weak insulating phase, we conclude that the electronic properties throughout the whole sample flake remain essentially homogeneous. Since the sample thickness is about 200 nm, much larger than the typical effective modulation depth of electrostatic double-layer gating (usually only a few nanometers [34–37]), we can reasonably attribute the gate-controlling effect in our iFET to Li ion doping rather than electrostatic charge accumulation. There is other evidence to support the electrochemical doping mechanism: the tuning process is not fully reversible if the V_g was overloaded. We can only restore the initial zero-bias resistance and superconductivity when V_g is swept back before reaching a threshold voltage $V_{\text{th}} \leq V_g^C + 0.3$ V. When V_g exceeds V_{th} , the insulating phase would be preserved even if V_g was swept back to zero or even -6 V, suggesting a chemical modification of (Li,Fe)OHFeSe. A detailed discussion of the effect of the applied gate voltage is presented in the Supplemental Material [16].

To further reveal the underlying electronic properties, we measured the temperature and gate-voltage dependence of Hall resistance R_{xy} as shown in Fig. 3(a). The transport properties of superconducting (Li,Fe)OHFeSe are dominated by electron-type carriers at low temperatures. At $V_g = 0$ V, R_H shows a flat minimum at around 75 K, then increases slightly with decreasing temperature. As V_g is raised up to 3.6 V, this minimum disappears, and for the optimal gating $V_g = 3.9$ V ($T_c^{\text{mid}} = 43.4$ K), R_H decreases rapidly toward T_c . The low-temperature downturn of R_H has also been observed in $\text{K}_x\text{Fe}_{2-y}\text{Se}_2$ single crystals with $T_c = 32$ K [38]. In addition, the evolution of R_H - T curves from an undoped ($V_g = 0$ V) to an optimally doped ($V_g = 3.9$ V) sample mimics that of one-unit-cell FeSe films on SrTiO₃ substrate with annealing time prolonged from 20 to 42 h [22]. This similarity may hint at some universal feature in these high- T_c Fe-chalcogenide superconductors. In the insulating regime, the field dependence of $R_{xy}(H)$ becomes nonlinear and dominated by hole-type carriers (see the Supplemental Material [16] for more details), being similar to the behavior of bulk β -FeSe [21]. The sign reversal and strong temperature dependence of R_H in SC samples, as well as the nonlinear $R_{xy}(B)$ in the insulating phase, is evidence of the multiband effect. These observations indicate the coexistence of electron and hole carriers in (Li,Fe)OHFeSe on both sides of the superconductor-insulator transition, which also suggests that the insulating phase is likely to be induced by carrier localization effect.

In Fig. 3(b), we plot R_H and Hall number $n_H = 1/eR_H$ as a function of V_g at $T = 70$ K. We note that the Hall number per Fe site of the conducting FeSe layer [Fe(2) site] is appreciable, and thus could not represent the actual doping level. Similar to many of the iron-based superconductors [30,39], R_H in

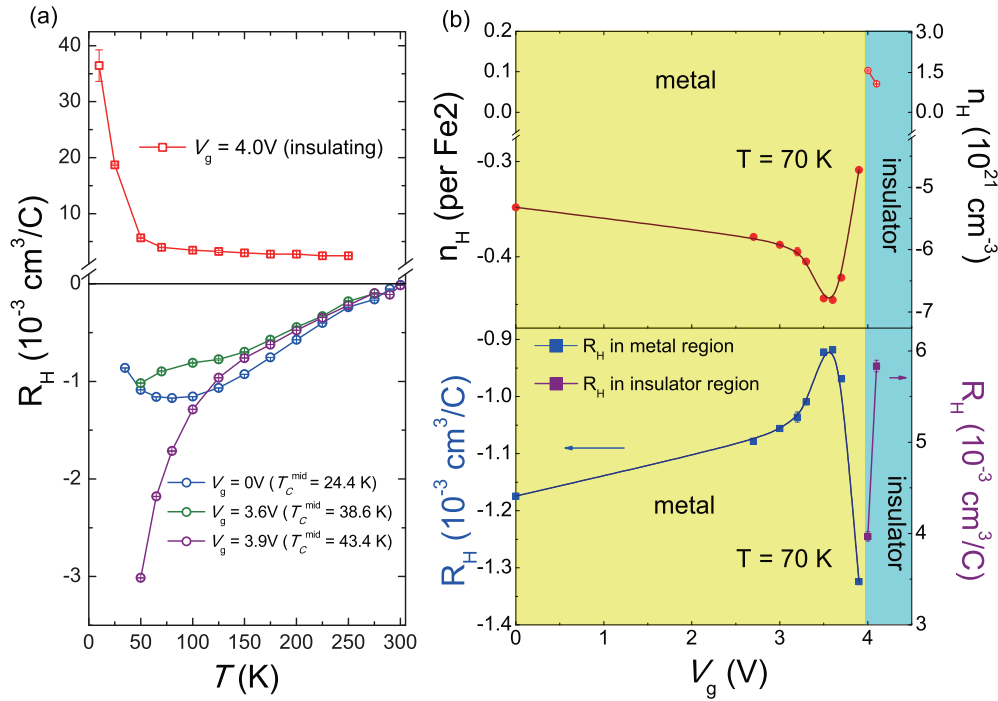


FIG. 3. (a) Temperature dependence of Hall coefficient R_H at different gate voltages. The thickness (t) of the measured (Li,Fe)OHFeSe flake is 210 nm. $R_H = (R_{xy}/B)t$ was calculated by linear fitting of R_{xy} versus B plot from -5 to 5 T in the superconducting phase, and linear fitting of R_{xy} from 2.5 to 9 T after subtracting the zero-field value in the insulating phase (see the Supplemental Material [16]). Error bars represent the uncertainty of linear fitting. (b) The lower and upper panels show the Hall coefficient R_H and Hall number $n_H = 1/R_H e$ as a function of V_g at 70 K , respectively. Hall number per Fe site in the FeSe layer was calculated based on the unit-cell volume reported in Ref. [9]. The filled and open circles correspond to the electron-type and hole-type carriers, respectively.

(Li,Fe)OHFeSe could be significantly reduced owing to the compensating effect between different bands. Upon applying V_g , R_H initially increases in accord with an electron doping process. At $V_g = 3.8 \text{ V}$, where T_c^{mid} increases to 38.6 K , R_H reaches a maximum where the Hall number n_H suggests an extra doping of $\simeq 0.1e$ per Fe(2) site compared to the ungated state. With further increasing V_g , the optimal T_c can be achieved, whereas R_H decreases drastically, being consistent with the low-temperature downturn of R_H in the near optimally gated sample in Fig. 3(a). Referring to the obviously reduced low-temperature resistance in this gate-voltage range (Fig. 2), we attribute this feature to the enhanced electron mobility near the optimal doping. The most remarkable part in our data is the sudden sign change of R_H across the boundary of the superconductor-insulator (S-I) transition, evidence of the dramatic modification in the electronics across the phase boundary.

Despite the difficulties of characterizing the iFET *in situ* during the gate-voltage tuning process, some findings are helpful for the understanding of the origin of the S-I transition and the nature of the gate modulation mechanism. The experimental evidence suggests a gate-controlled lithiation scenario: (i) Below $V_{\text{th}} > V_g^C$, the transition is reversible, and we can drive the iFET to go through the phase boundary repeatedly (see Supplemental Material [16]), which distinguishes the S-I transition from the possible sample degradation. (ii) In the samples with irreversible insulating behavior, we could find neither detectable shifting ($> 0.01^\circ$) of x-ray diffraction peaks nor new Raman modes (see Supplemental Material [16]).

These results unambiguously rule out the possibility of both degradation and Li ion intercalation into the space between the hydroxide layer and FeSe layer. (iii) The SC transition width is obviously reduced approaching the optimal T_c , indicating the improvement of sample homogeneity upon gate modulating in the SC regime.

Based on these findings, we propose a scenario of the lithiation process. First, the Li ions in the electrolyte enter the iFET and displace the iron atoms in the (Li,Fe)OH space layer; the displaced Fe atoms can migrate to the adjacent FeSe layer and fill the vacancies. In this step, the average electron count per iron site in the FeSe layer increases [18]. Both the reduction of the vacancy concentration and the electron doping can contribute to the enhancement of T_c . Similar controlling of T_c by slightly changing the $\text{Li}^+/\text{Fe}^{2+}$ ratio in the hydroxide layer has been reported in powder samples [18,40]. As most of the vacancies are filled, the samples achieve the optimal $T_c = 43.4 \text{ K}$ at $V_g = V_g^C$ and become almost homogeneous as indicated by the sharp superconducting transition. Between V_g^C and V_{th} , the (Li,Fe)OHFeSe thin flakes suddenly become insulating, which is very surprising. While V_g continues ramping up beyond V_{th} , Li ions may start to replace the Fe atoms in FeSe plane. Because the “displaced out” Fe ions have a much lower mobility than the Li ions in the electrolyte, they can hardly reenter the lattice and reoccupy the original sites when V_g was swept back, which eventually results in an irreversible state. In the phase diagram [Fig. 4(a)], V_g is used merely as a nominal parameter, because the carrier concentration and the substitution of Li for Fe cannot be clearly quantified.

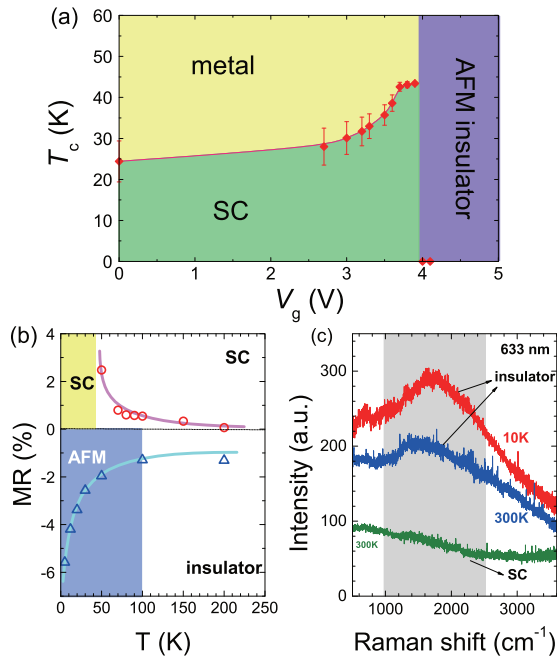


FIG. 4. (a) Phase diagram of electronic phases as a function of gate voltage V_g for (Li,Fe)OHFeSe. The boundary of SC phase and metal phase is determined by the midpoint critical temperature T_c^{mid} . Error bars are defined as the width of SC transition. (b) Transverse magnetoresistance (TMR) of a superconducting (Li,Fe)OHFeSe iFET (red circle) and an insulating (Li,Fe)OHFeSe iFET (blue triangle), as a function of temperature. The superconducting iFET is tuned to $T_c = 42$ K. For both samples, the TMR was measured with the applied magnetic field parallel to the c direction. The solid lines are guides to the eye. (c) Two-magnon Raman spectra for superconducting and insulating (Li,Fe)OHFeSe. Red and blue solid lines stand for the Raman spectra for insulating (Li,Fe)OHFeSe at 10 and 300 K, respectively. The olive solid line stands for Raman spectrum at 300 K for superconducting (Li,Fe)OHFeSe with $T_c^{\text{mid}} = 24.4$ K. The gray area is the region for two-magnon mode.

The phase diagram of gate-voltage-modulated (Li,Fe)OHFeSe iFET is depicted in Fig. 4(a). Two distinct phase regimes, the metallic phase with superconductivity emerging at low temperatures and the insulating phase, are separated by a sharp phase boundary located at $V_g = V_g^C \simeq 4$ V without any evident coexistence. The abrupt disappearance of T_c and discontinuity of R_H at the phase boundary indicate a first-order character of this gate-voltage-induced S-I phase transition. In analogy with other unconventional superconductors induced by doping a parent compound, the phase diagram could be interpreted by doping holes into the insulating phase that is in the gating voltage range from V_{th} to V_g^C . In a reversible cycle, by tuning the gate voltage from V_{th} to V_g^C and lower value, the driven-out Li ions from the crystals can effectively dope holes into the electronic system, and eventually makes the insulating state melt down and gives rise to superconductivity.

To understand the nature of the insulating phase, the transverse magnetoresistance (TMR) and electronic Raman scattering measurements on the insulating phase are carried out. As shown in Fig. 4(b), in a superconducting iFET

with nearly optimal T_c (42 K), the TMR is positive at all temperatures, which can reasonably be attributed to the orbital magnetoresistance (MR) [41]. For the insulating phase, however, a negative transverse MR is observed within the entire temperature range, with an accelerated enhancement below 100 K (MR curves are shown in Supplemental Material Fig. S8 [16]). Negative MR usually reflects the reduction of spin scattering [42] or a suppression of the spin fluctuations [41] by the external field. A similar negative MR was also reported in the weak insulating antiferromagnetic state of lightly doped cuprates and was explained as the spin-related effects [43]. The electronic Raman spectra of an insulating (Li,Fe)OHFeSe sample (after an irreversible gating cycle) are shown in Fig. 4(c). A broad and asymmetric peak can be clearly seen around 1600 cm^{-1} at 10 K and such peak is also distinguishable with a reduced intensity, and slightly shifts to low frequency at 300 K. The peak position, asymmetry, and width for the peak around 1600 cm^{-1} are all consistent with two-magnon excitations, which can be simply described as simultaneous excitations of a magnon defined in the two spin sublattices of an antiferromagnetic (AFM)/spin-density-wave (SDW) system. The two-magnon process is a fundamental technique in probing magnetic excitations, and has been proved to be effective in studying the magnetic order in the parent compounds of cuprate superconductors [44,45]. In fact, the two-magnon process has also been theoretically analyzed [46] as well as experimentally observed in Fe(Se,Te)-based compounds [47,48]. In shape contrast to the insulating (Li,Fe)OHFeSe sample, the two-magnon excitation is absent in the superconducting (Li,Fe)OHFeSe sample as shown in Fig. 4(c). These results indicate that AFM order/fluctuation or the amplitude of local moment is strongly enhanced through the superconductor-insulator transition observed in the present work. Both the TMR and the electronic Raman results of the insulating (Li,Fe)OHFeSe sample hint that a possible AFM/SDW state may exist in the insulating (Li,Fe)OHFeSe although direct evidence for static order or phase transition for AFM/SDW is still lacking in current stage.

In summary, we report the appearance of an insulating phase with AFM order/fluctuation immediately adjacent to the optimal superconductivity in iron-based superconductor (Li,Fe)OHFeSe. Similar phase diagrams have been observed in the two-dimensional organic superconductors and Cs_3C_{60} . This phase diagram of FeSe-derived superconductors also bears a resemblance to that of high- T_c cuprate superconductors. The similarity of these phase diagrams transcends the diversity of various unconventional superconducting materials, suggesting that all of them share a universal mechanism in superconductivity. Our finding in (Li,Fe)OHFeSe iFET helps to unify the underlying physics in both the cuprates and FeSe-derived materials. Moreover, our work suggests that the gate-controlled strong charge doping is a very powerful practice for the exploration of novel states of matter that cannot be realized using traditional methods.

We would like to thank Yuanbo Zhang for discussions on ionic liquid gating, and thank Liangjian Zou for discussions on Raman scattering. This work is supported by the National Natural Science Foundation of China (Grants No. 11190021,

No. 11534010 and No. 91422303), the “Strategic Priority Research Program (B)” of the Chinese Academy of Sciences (Grant No. XDB04040100), the National Basic Research Program of China (973 Program, Grant No. 2012CB922002), and Hefei Science Center CAS (2015SRG-HSC013). Partial

work was done in USTC Center for Micro and Nanoscale Research and Fabrication at USTC, Hefei, Anhui. Q.Z. was supported by the National Basic Research Program of China (973 Program, Grant No. 2012CB921701) and the National Natural Science Foundation of China.

-
- [1] P. A. Lee, N. Nagaosa, and X. G. Wen, *Rev. Mod. Phys.* **78**, 17 (2006).
- [2] K. Miyagawa, A. Kawamoto, Y. Nakazawa, and K. Kanoda, *Phys. Rev. Lett.* **75**, 1174 (1995).
- [3] S. Lefebvre, P. Wzietek, S. Brown, C. Bourbonnais, D. Jérôme, C. Mézière, M. Fourmigué, and P. Batail, *Phys. Rev. Lett.* **85**, 5420 (2000).
- [4] F. Kagawa, K. Miyagawa, and K. Kanoda, *Nature (London)* **436**, 534 (2005).
- [5] Y. Takabayashi, A. Y. Ganin, P. Jeglič, D. Arčon, T. Takano, Y. Iwasa, Y. Ohishi, M. Takata, and K. Prassides, *Science* **323**, 1585 (2009).
- [6] A. J. Drew, Ch. Niedermayer, P. J. Baker, F. L. Pratt, S. J. Blundell, T. Lancaster, R. H. Liu, G. Wu, X. H. Chen, I. Watanabe, V. K. Malik, A. Dubroka, M. Rössle, K. W. Kim, C. Baines, and C. Bernhard, *Nat. Mater.* **8**, 310 (2009).
- [7] J. Zhao, Q. Huang, Clarina de la Cruz, S. L. Li, J. W. Lynn, Y. Chen, M. A. Green, G. F. Chen, G. Li, Z. Li, J. L. Luo, N. L. Wang, and P. C. Dai, *Nat. Mater.* **7**, 953 (2008).
- [8] H. Chen, Y. Ren, Y. Qiu, W. Bao, R. H. Liu, G. Wu, T. Wu, Y. L. Xie, X. F. Wang, Q. Huang, and X. H. Chen, *Europhys. Lett.* **85**, 17006 (2009).
- [9] X. F. Lu, N. Z. Wang, H. Wu, Y. P. Wu, D. Zhao, X. Z. Zeng, X. G. Luo, T. Wu, W. Bao, G. H. Zhang, F. Q. Huang, Q. Z. Huang, and X. H. Chen, *Nat. Mater.* **14**, 325 (2015).
- [10] W. Li, H. Ding, P. Deng, K. Chang, C. L. Song, K. He, L. L. Wang, X. C. Ma, J. P. Hu, X. Chen, and Qi-Kun Xue, *Nat. Phys.* **8**, 126 (2012).
- [11] C. H. Ahn, J. M. Triscone, and J. Mannhart, *Nature (London)* **424**, 1015 (2003).
- [12] C. H. Ahn, A. Bhattacharya, M. Di Ventura, J. N. Eckstein, C. Daniel Frisbie, M. E. Gershenson, A. M. Goldman, I. H. Inoue, J. Mannhart, Andrew J. Millis, Alberto F. Morpurgo, Douglas Natelson, and Jean-Marc Triscone, *Rev. Mod. Phys.* **78**, 1185 (2006).
- [13] R. E. Glover and M. D. Sherrill, *Phys. Rev. Lett.* **5**, 248 (1960).
- [14] C. H. Ahn, S. Gariglio, P. Paruch, T. Tybell, L. Antognazza, and J.-M. Triscone, *Science* **284**, 1152 (1999).
- [15] Y. J. Yu, F. Y. Yang, X. F. Lu, Y. J. Yan, Yong-Heum Cho, L. G. Ma, X. H. Niu, S. Kim, Young-Woo Son, D. L. Feng, S. Y. Li, Sang-Wook Cheong, X. H. Chen and Y. B. Zhang, *Nat. Nanotechnol.* **10**, 270 (2015).
- [16] See Supplemental Material at <http://link.aps.org/supplemental/10.1103/PhysRevB.93.060501>, which includes Refs. [17–33], for more details about the gate-tuned superconductivity and the insulating phase.
- [17] X. F. Lu, N. Z. Wang, G. H. Zhang, X. G. Luo, Z. M. Ma, B. Lei, F. Q. Huang, and X. H. Chen, *Phys. Rev. B* **89**, 020507(R) (2014).
- [18] H. L. Sun, D. N. Woodruff, S. J. Cassidy, G. M. Allcroft, S. J. Sedlmaier, A. L. Thompson, P. A. Bingham, S. D. Forder, S. Cartenet, N. Mary, S. Ramos, F. R. Foronda, B. H. Williams, X. D. Li, S. J. Blundell, and S. J. Clarke, *Inorg. Chem.* **54**, 1958 (2015).
- [19] F. Rullier-Albenque, D. Colson, A. Forget, P. Thuéry, and S. Poissonnet, *Phys. Rev. B* **81**, 224503 (2010).
- [20] F. Rullier-Albenque, D. Colson, A. Forget, and H. Alloul, *Phys. Rev. Lett.* **103**, 057001 (2009).
- [21] H. C. Lei, D. Graf, R. W. Hu, H. Ryu, E. S. Choi, S. W. Tozer, and C. Petrovic, *Phys. Rev. B* **85**, 094515 (2012).
- [22] W. H. Zhang, Z. Li, F. S. Li, H. M. Zhang, J. P. Peng, C. J. Tang, Q. Y. Wang, K. He, X. Chen, L. L. Wang, X. C. Ma, and Q.-K. Xue, *Phys. Rev. B* **89**, 060506(R) (2014).
- [23] J. N. Reimers and J. R. Dahn, *J. Electrochem. Soc.* **139**, 2091 (1992).
- [24] D. Aurbach and Y. Ein-Eli, *J. Electrochem. Soc.* **142**, 1746 (1995).
- [25] G. Vitins and K. West, *J. Electrochem. Soc.* **144**, 2587 (1997).
- [26] R. J. Nemanich, S. A. Solin, and D. Gérard, *Phys. Rev. B* **16**, 2965 (1977).
- [27] M. Inaba, H. Yoshida, Z. Ogumi, T. Abe, Y. Mizutani, and M. Asano, *J. Electrochem. Soc.* **142**, 20 (1995).
- [28] R. Baddour-Hadjean, V. Golabkan, J. P. Pereira-Ramos, A. Mantoux, and D. Lincot, *J. Raman Spectrosc.* **33**, 631 (2002).
- [29] T. Sekine, C. Julien, I. Samaras, M. Jouanne, and M. Balkanski, *Mater. Sci. Eng. B* **3**, 153 (1989).
- [30] F. Rullier-Albenque, D. Colson, A. Forget, and H. Alloul, *Phys. Rev. Lett.* **109**, 187005 (2012).
- [31] M. L. Amigó, V. A. Crivillero, D. G. Franco, and G. Nieva, *J. Phys.: Conf. Ser.* **568**, 022005 (2014).
- [32] Y. Toyozawa, *J. Phys. Soc. Jpn.* **17**, 986 (1962).
- [33] H. Yamada and S. Takada, *J. Phys. Soc. Jpn.* **34**, 51 (1973).
- [34] J. T. Ye, S. Inoue, K. Kobayashi, Y. Kasahara, H. T. Yuan, H. Shimotani, and Y. Iwasa, *Nat. Mater.* **9**, 125 (2010).
- [35] K. Ueno, S. Nakamura, H. Shimotani, A. Ohtomo, N. Kimura, T. Nojima, H. Aoki, Y. Iwasa, and M. Kawasaki, *Nat. Mater.* **7**, 855 (2008).
- [36] K. Ueno, S. Nakamura, H. Shimotani, H. T. Yuan, N. Kimura, T. Nojima, H. Aoki, Y. Iwasa, and M. Kawasaki, *Nat. Nanotechnol.* **6**, 408 (2011).
- [37] A. T. Bollinger, G. Dubuis, J. Yoon, D. Pavuna, J. Misewich, and I. I. Božović, *Nature (London)* **472**, 458 (2011).
- [38] X. X. Ding, Y. M. Pan, H. Yang, and H.-H. Wen, *Phys. Rev. B* **89**, 224515 (2014).
- [39] K. Ohgushi and Y. Kiuchi, *Phys. Rev. B* **85**, 064522 (2012).
- [40] X. L. Dong, H. X. Zhou, H. X. Yang, J. Yuan, K. Jin, F. Zhou, D. N. Yuan, L. L. Wei, J. Q. Li, X. Q. Wang, G. M. Zhang, and Z. X. Zhao, *J. Am. Chem. Soc.* **137**, 66 (2015).
- [41] F. Rullier-Albenque, D. Colson, and A. Forget, *Phys. Rev. B* **88**, 045105 (2013).
- [42] V. P. Jovanović, L. Fruchter, Z. Z. Li, and H. Raffy, *Phys. Rev. B* **81**, 134520 (2010).

- [43] V. N. Kotov, O. P. Sushkov, M. B. Silva Neto, L. Benfatto, and A. H. Castro Neto, *Phys. Rev. B* **76**, 224512 (2007).
- [44] R. R. P. Singh, P. A. Fleury, K. B. Lyons, and P. E. Sulewski, *Phys. Rev. Lett.* **62**, 2736 (1989).
- [45] G. Blumberg, P. Abbamonte, M. V. Klein, W. C. Lee, D. M. Ginsberg, L. L. Miller, and A. Zibold, *Phys. Rev. B* **53**, R11930(R) (1996).
- [46] C.-C. Chen, C. J. Jia, A. F. Kemper, R. R. P. Singh, and T. P. Devereaux, *Phys. Rev. Lett.* **106**, 067002 (2011).
- [47] K. Okazaki, S. Sugai, S. Niitaka, and H. Takagi, *Phys. Rev. B* **83**, 035103 (2011).
- [48] A. M. Zhang, J. H. Xiao, Y. S. Li, J. B. He, D. M. Wang, G. F. Chen, B. Normand, Q. M. Zhang, and T. Xiang, *Phys. Rev. B* **85**, 214508 (2012).